NASA TECHNICAL MEMORANDUM TM-88427

FORMATION OF THE CENTRAL UPLIFT IN METEORIC CRATERS

Ivanov, B.A.; Bazilevskiy, A.T.; Sazonova, L.V.

Translation of "Ob obrazovanii tsentralnogo podnyatiya v meteoritnykh krateraxh," in "Meteoritika, Akademiya nauk SSSR" No. 40, 1982, pp. 67-81

NATIONAL AERONAUTICS AND SPACE ADMINISTRATION
WASHINGTON, D.C. 20546 MAY, 1986

FORMATION OF THE CENTRAL UPLIFT IN METEORIC CRATERS

V.A. Ivanov

INTRODUCTION

/67*

Central peaks or central uplifts in meteoric craters are a necessary element in the structure of craters in a certain size range, e.g. craters with a diameter of 25-200 km on the Moon and 4-70(?) km on Earth. Smaller craters have a simple cup shape; larger craters are complex multiringed structures. The transition from simple cup-shaped craters to craters with central uplifts is associated with a decrease in relative crater depth, which brings into question the depth of excavation during formation of craters with complex structure. A change in crater structure indicates a change in the mechanics of crater formation and requires caution when one attempts to extrapolate to natural occurrences the set of data accumulated during study of this process using experimental explosions and hypervelocity impacts under laboratory conditions.

The purpose of this article is to discuss and, if possible, evaluate the relationship of various processes which accompany crater formation; to attempt to identify those which can be related to the natural appearance of central uplifts in impact craters on a certain scale.

Since formation of simple, cup-shaped craters has been studied most thoroughly, we will use certain relationships established for them in the first approximation over the entire range of structures studied. Thus, this article may in some places seem to be a "reductio ad absurdum" of data on crater

*Numbers in the margin indicate pagination of the foreign text.

formation on a small scale, which, in and of itself, is useful for identifying the least studied aspects of crater formation.

OBSERVATIONS

Let us consider factual data on craters with central uplifts on various planetary bodies.

Earth. We know that proven meteoric craters on the Earth's surface include craters at various levels of preservation. Therefore, judgments about the initial structure of craters of a different scale are usually made using the example of a small number of best preserved structures. Craters less than 3-4 km in diameter have simple cup-shaped structures [Masaytis, 1971; Dence, et al., 1977]. Well preserved craters larger than 3-4 km in diameter are depressions with a central uplift. These include the relatively well studied structures of the Steinheim (FRG, $D \approx 4$ km), Boltyshsk (UkSSR, $D \approx 25$ km), and Kara (Polar Urals, USSR, $D \approx 50$ km) craters. Along with a possible central uplift, larger craters exhibit concentric elevated rings, such as, for example, in the Popigay crater (USSR, $D \approx 100$ km) [Masaytis et al., 1975].

In well preserved craters, one can trace certain quantitative characteristics of central uplifts. Let us introduce the following identifications (fig. 1): D - crater diameter; H_1 - depth from original surface to visible crater bottom; H_2 - depth from original surface to true crater bottom (disregarding the cover of allogenous breccia); h - height of the central uplift over the visible crater bottom; h_1 - height of the central uplift over the true crater bottom; d - depth of the apex of the central uplift relative to the level of the initial surface (if the central uplift projects above the original level, d is less than 0). /68

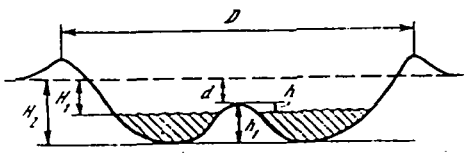

Fig. 1. Elements of the structure of a typical crater with central uplift.

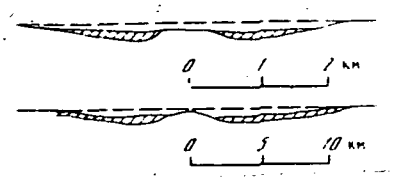

Fig. 2. Simplified diagram of the structure of Steinheim (top) and Boltyshsk (bottom) meteoric craters.

Figure 2 shows simplified diagrams of the structure of the Steinheim and Boltyshsk craters [Reiff, 1977; Yurk et al., 1975]. Table 1 shows their dimensions, as well as data on the amplitude of rock uplift Δz above the original occurrence, obtained for central uplifts of several eroded craters.

It is important to note that, if there are noticeable amounts of impact melting in the crater, it is never found at the apex of the central uplift. As a rule, it forms a bed around the central uplift [Masaytis, 1977].

TABLE 1

LINEAR DIMENSIONS (IN KM) OF CERTAIN TERRESTRIAL METEORIC CRATERS WITH CENTRAL UPLIFTS

1) Кратер	D	H_1	H_2	h	h_1	d	Δz	3) Литература
Steinheim	4	0,17	0,20	0,1	0,13	0,07	0,13	Reiff, 1977
Flynn-Creek	4	0,1	0,12	0,11	0,11	0 (?)	0,4	Roddy, 1977
Decaturville	6	–	–	–	–	–	0,3–0,5	Offield, Pohn, 1977
Sierra Madera	13	–	–	–	–	–	1	Dence et al., 1977
Gosses Bluff	20	–	–	–	–	–	2,5–3	Milton et al., 1972
2) Болтышский	25	0,5	1,0	0,1	0,6	0,4	2*	4) Юрк и др., 1975

*Amplitude of the elevation of the central uplift, estimated in terms of minimum depth of the impact melt zone, z'_m (see table 3).

Key: 1) Crater; 2) Boltyshsk 3) Reference; 4) Yurk et al.

TABLE 2

CERTAIN CHARACTERISTICS OF PLANAR ELEMENTS IN QUARTZ SAND FROM THE CORE OF A BOREHOLE DRILLED IN THE CENTRAL UPLIFT OF THE KARA CRATER

1) Глубина залегания образца	2) Доля зерен с планарными деформациями, %	Доля зерен с различными типами планарных элементов, % 3)				Доля зерен с микротрещинами кливажа, % 4)	Давление 5) ударной волны, кбар
		A	B	C	D		
72–100	100	3	36,5	18	30,5	12	120
292	97	26	63	–	4	4	93
315–373	88	12	46	3	12	15	93
391–429	84	24	49	6	1	4	88
434–472	80	23	44	4	8	1	90
483–535	72	25	32	3	10	2	87
548–584	73	26	27	2	13	5	87
590–614	51	14,5	16	4	12	4	82

Key: 1) Depth of sample deposit; 2) Percentage of grain with planar deformations; 3) Percentage of grain with various types of planar elements; 4) Percentage of grain with cleavage microcracks; 5) Shock wave pressure, kbar.

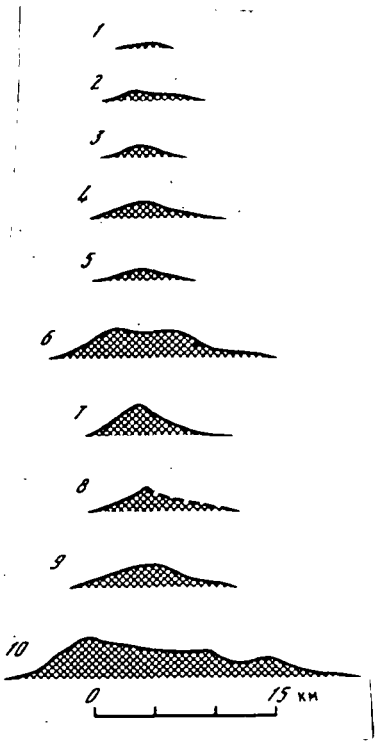

Fig. 3. Profiles of central peaks /69 for a series of lunar craters. The level of the flat crater bottom is taken as the foot; Crater names and diameters in km: 1) Van Fleck, 35.8; 2) Beck, 35.8; 3) Pliny, 42.1; 4) Bruner, 51.6; 5) Schubert, 53.9; 6) King, 78; 7) Theophilus, 102; 8) Aitken, 137; 9) Neper, 148.5; 10) Tsiolkovskiy, 197.

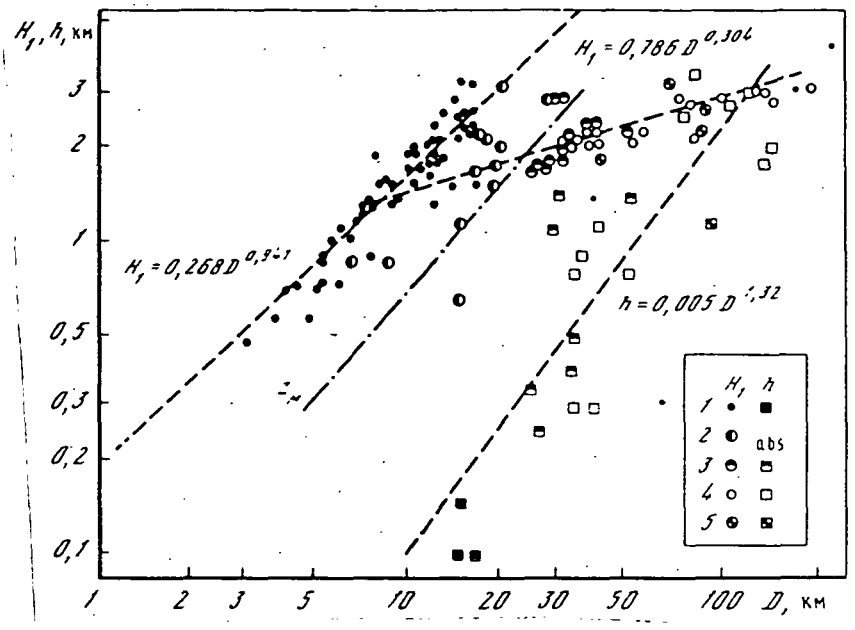

Fig. 4. Crater depth and central peak height as a function of diameter on the Moon.
Crater types: 1) Schmidt; 2) Dawes; 3) Remer; 4) Tycho; 5) Copernicus. The dot-dash line represents the estimated depth of the melt zone z_M [11].

For certain craters there is a known level of impact metamorphism of rock in the upper part of the central uplift. This makes it possible to calculate pressure at the shock wave front. The largest known well preserved crater with central uplift on Earth is the Kara [Maslov, 1977]. Work done on this crater has made it possible to determine the degree of impact metamorphism in quartz sand from central uplift rock. Core samples from boreholes were used to obtain samples from the following depth ranges: 72-100, 292, 315-373, 391-429, 434-472, 483-535, 590-614 m. Quartz sand exhibited both planar elements and cleavage cracks. Angles between the normal to planar distortion and axis C were measured. For each depth range, 100-300 measurements were taken. The method proposed in the article [Robertson, 1975] was used to classify the quartz sand into four types depending on the preferred direction of development of planar elements: A, B, C, and D. Pressures in

the shock waves acting on these grains at the original deposits of rock now constituting the central uplift were calculated in terms of the relative proportion of a particle grain type. Table 2 shows the results of these measurements. It is obvious that pressure in the shock wave near the apex of the central uplift is no more than 120 kbar and diminishes slowly with depth, as is natural given the existing ratio of total borehole length (0.5 km) to crater diameter (50 km).

/70

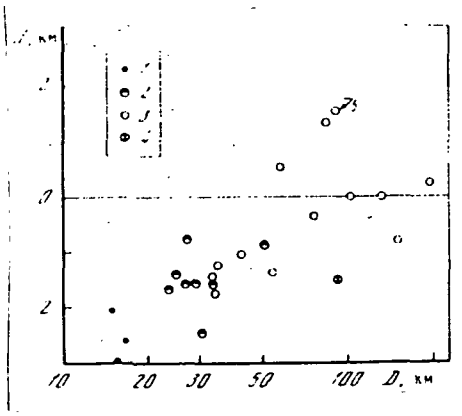

Fig. 5. Height of the apex of a lunar crater peak relative to the original surface level. Crater types: 1) Schmidt; 2) Remer; 3) Tycho (5 - crater Icarus); 4) Copernicus.

Moon. As regards fresh Moon craters, it has been possible to identify several morphological crater types which regularly succeed one another as diameter increases: Schmidt, or cup-shaped (D smaller than 10-15 km); Dawes (D = 10-25 km), Remer (D = 25-50 km); Tycho and Copernicus (D = 35-200 km), concentric basins (D greater than 200 km) [Florensky et al., 1976]. Complex craters have a small relative depth, so that the ratio of crater depth to diameter diminishes even more as diameter increases, and there is a shift from Dawes- to Remer-type craters and then to Tycho- and Copernicus-type.

Central peaks are a necessary element in the structure of Remer-, Tycho-, and Copernicus-type craters. Positive reliefs in the form of mounds and ridges are never called central peaks, but they are typical for Dawes-type craters. Atypical central peaks exist in craters 14-16 km in diameter, e.g. in the crater Hill, which gravitate toward the cup-shaped

crater group because of their characteristics. When differentiated according to the extent to which they are delineated in craters of the same size, central peaks have a tendency to be more clearly delinated in large craters (cf. fig. 3). The height of a central peak above the visible crater bottom rises as its diameter increases (fig. 4).

Note that combined functions $H_1(D)$ and $h(D)$ intersect at a diameter of about 130 km. This means that in large-diameter craters the central peak should generally extend above the original surface level.

For several craters, LTO-series maps made it possible to trace the depth of the apex of a central uplift as a function of crater diameter. These data (fig. 5) demonstrate that the depth of the central uplift apex diminishes to zero as crater diameter increases, and then the apex of the peak is higher then the level of the original surface. The case of a central peak towering above the wall of a crater has been noted (crater Icarus, D = 90 km) [Allen, 1975].

Mercury. Mercury's young craters include all the lunar crater types mentioned above. However, their evolution on Mercury takes place at smaller crater sizes than on the Moon. This is usually attributed to the fact that the gravitational force on the Moon is twice as great. The diameters of various types of craters vary in the following ranges: cup-shaped, D less than 7; Dawes, D = 7-15; Remer, D = 10-20; Tycho and Copernicus, D = 15-30; concentric basins, D 100-130 km. Just as on the Moon, crater depth first increases directly with diameter (for cup-shaped craters), then abruptly slows exponentially with an exponent less than one [Gault et al., 1975].

Mars. Craters on Mars exhibit the same principles as those

on the Moon and Mercury. Threshold values for dimensions of various types of craters have still not been firmly established, but it is clear that they are a function of the properties of the rocks, which are much more diverse on Mars than on the Moon or Mercury. According to data from Wood [Wood et al., 1978], 100% of craters with diameter greater than 10 km in valleys and more than 15 km in cratered regions have central peaks. This is generally rather close to values for Mercury. The transition from simple to complex crater types on Mars is also associated with a decrease in their depth [Controlled Mosaics, 1977].

Phobos. Phobos has few craters of the diameter range considered (greater than 1-2 km). The average cross section of Phobos is close to 20 km. The largest crater (Stikni) has a diameter of about 10 km. Craters of all sizes with rather well preserved morphology have a cup shape. There is only one crater with a diameter of about 1.5 km with a clearly pronounced central peak. Thus, one may assert that Phobos /71
lacks the class of craters similar to Remer, Copernicus, and Tycho on the Moon and Mercury.

EVALUATIONS

Energy of a Crater-Forming Meteorite. To consider the relationship of various cratering parameters, it is convenient to use the kinetic energy KE of a meteorite forming a given crater. Although this figure and its relationship to the scale of the phenomenon are now being only rough evaluated, analyzing the observable characteristics of craters in terms of energy makes it possible to view them from a single standpoint.

One of the most common methods of evaluating KE with data on explosion cratering has already been used by many researchers [Shumeyker, 1968; Baldwin, 1963; Dence et al.,

1977]. An explosion of energy E at depth z such that the explosion crater's morphology was similar to the morphology of the given crater was used (cf. e.g. [Shumeyker, 1968; Oberbek, 1977]). Henceforth we will use the function proposed in [Dence et al., 1977] for terrestrial craters in crystalline rock:

$$D = 1{,}96 \cdot 10^{-5} KE^{3{,}4}, \tag{1}$$

where D is crater diameter along the crown of the wall, km; KE, kinetic energy of the meteorite, J. If we measure the explosive material's kinetic energy in megatons of TNT, then, considering that 1 Mt = 4.18×10^{15} J and transforming (1), we obtain

$$KE = 2{,}43 D^{3{,}4}. \tag{2}$$

Here and henceforth, KE will be expressed in Mt; D, in km.

If gravitational force differs from that on Earth, the relationship between kinetic energy and diameter for the entire range of crater sizes is still not certain. For large cup-shaped craters, there are both experimental [Johnson et al., 1969; Gault, Wedekind, 1977] and theoretical [Ivanov, 1976; Bazilevskiy, Ivanov, 1977; Maxwell, 1977; Ivanov, 1979a, b] evaluations. The idea behind theoretical analysis lies in the fact that an increase in the scale of an occurrence with gravitation force g constant is equivalent, within certain limits, to an increase in KE with the scale of the occurrence constant. The function KE(g,D) can be expressed as [Bazilevskiy, Ivanov, 1977; Ivanov 1979b]

$$KE \approx g^{N-3} D^N, \tag{3}$$

where N is, to a certain extent, an empirical coefficient. Although (3) is sufficiently valid for cup-shaped craters, we will assume it to be valid over the entire range of crater

diameters. This will make it possible to perform an evaluation in the zero approximation.

Reducing (2) to the form of (3) with regard for terrestrial $g = 9.81$ m/sec^2, we obtain

$$KE = 0{,}77\, g^{0{,}4} D^{3{,}4}. \tag{4}$$

Applying (4) to lunar conditions ($g = 1.62$ m/sec^2), we have

$$KE = 0{,}9\, D^{3{,}4}. \tag{5}$$

Shock Wave Attenuation. Calculation. Figure 6 shows the results of calculating shock wave attenuation in rock upon impact of meteorites of different composition traveling at different speeds. The simple principle of energy similitude and the relationship between maximum pressure at a shock front p and adjusted depth under the impact point $z/KE^{1/3}$ were used to compare data. Given these assumptions, as fig. 6 shows (thick line), data on shock wave attenuation in hypervelocity impacts against rock can be combined into the following equation

$$p = 0{,}2\, KE^{0{,}9} z^{-2{,}7}, \tag{6}$$

where p is measured in kbar; KE, in Mt; z, in km.

A change in the numerical coefficient in (6) from 0.1 to 0.4 (functions like (6) with these coefficient values are depicted in fig. 6 by thin lines) cover virtually all calculation points at impact velocities greater than 15 m/sec.

Note that fig. 6 presents data both with regard for phase shift in rock [Ahrens, O'Keefe, 1977] and disregarding it [O'Keefe, Ahrens, 1977; Bjork, 1961]. At impact velocities greater than 15 km/sec, data on shock wave attenuation correlate well among themselves and with data on shock wave attenuation in an aluminum target [Dienes, Walsh, 1969]. In /72

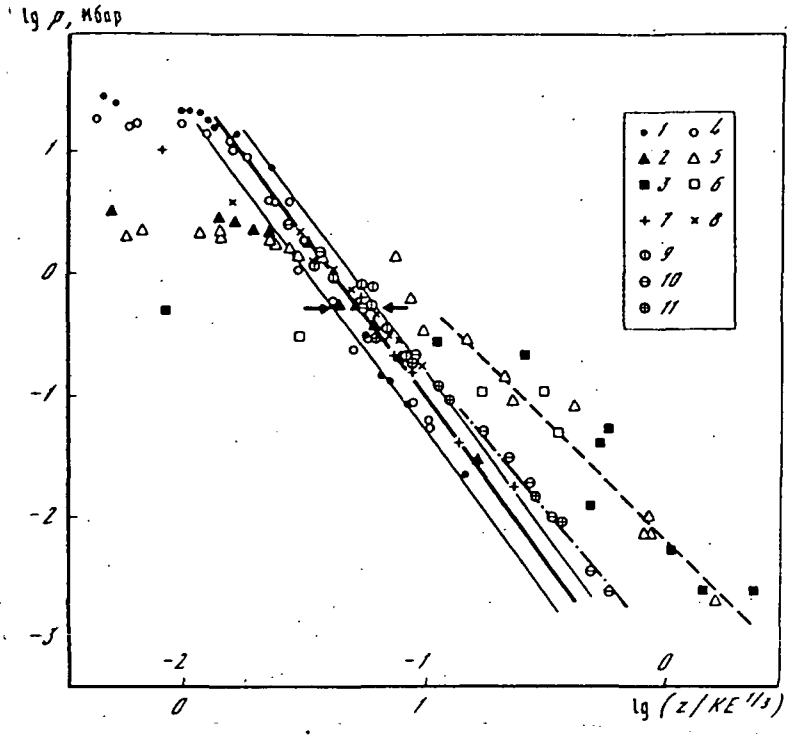

Fig. 6. Numerical modeling of attenuation of shock waves beneath the center of a crater.
The impact of a meteorite against an anorthosite target (Fe An) [Ahrens, O'Keefe, 1977] with velocities:
1) 45; 2) 15; 3) 5 km/sec; An An: 4) 45; 5) 15; 6) 5 km/sec (calculated with regard for phase shift in the target material); 7) Fe An, 15 km/sec [O'Keefe, Ahrens, 1977]; 8) Fe → tuff, 30 km/sec [Bjork, 1961]. For comparison, data from calculating the impact of aluminum against aluminum [Dienes, Walsh, 1969] at a velocity of 9) 80.4; 10) 24.3; 11) 7.3 km/sec are shown. Solid arrows indicate approximate pressure upon discharge of which rock begins to melt. The x-axis shows $km/Mt^{1/3}$ on the upper scale; $m/kt^{1/3}$ on the lower.

view of this correspondence, the results presented in [Ahrens, O'Keefe, 1977] for iron and stone strikers at 5 km/sec and for a stone striker at 15 km/sec are somewhat strange and incomprehensible. They show a shock wave attenuation anomalously weak as compared to other data. These data form a separate family of points denoted in fig. 6 by the broken

line. Volume of impact melt. One of the few means of checking evaluations of kinetic energy of crater-forming meteorites is to compare calculated and observed amounts of impact melting of rock in steep terrestrial meteoric craters. We know that rock such as granite is fusible after a shock wave with a maximum pressure of about 600 kbar passes through it. (This pressure, which we used for calculations, is indicated by arrows in fig. 6.) Then, from equation (6), one can determine the depth of the melt zone (in km):

$$z_M = 0{,}0515\, KE^{1/3}. \tag{7}$$

Using relationship (2) between meteorite kinetic energy and crater size under terrestrial conditions, we obtain

$$z_M = 0{,}07\, D^{1{,}13}. \tag{8}$$

Let us assume that the shape of the melt zone corresponds to a hemisphere of radius z_M, although this obviously somewhat overstates the volume of the melt zone. However, if we take into account the overall indeterminateness of our evaluations, this overstatement does not exceed the limits of overall calculating accuracy. Then the volume of the rock melting zone (in km^3) can be expressed as /73

$$V_M = \frac{2}{3}\pi z_M^3 = 0{,}7 \cdot 10^{-3} D^{3{,}4}. \tag{9}$$

which can be compared with Dence's calculation [1968]

$$V_M = 2 \cdot 10^{-3} D^3. \tag{10}$$

For craters with D = 10 km, equation (9) gives a melt volume equal to 1.73 km^3, which does not correlate well with that determined from equation (10), 2 km^3.

The results of evaluation with (9) have been collected in table 3 and compared with data from geological observations.

TABLE 3

EVALUATIONS OF MELT VOLUME FOR
CERTAIN TERRESTRIAL METEORIC CRATERS

1) Кратер	D, км	KE, Мт	$z_м$, км	$V_м = \frac{2}{3}\pi z_м$, км³	$V'_м$, км³	$z'_м = \sqrt{\frac{3V'_м}{2\pi}}$, км	3) Литература
Brent	3,8	227	0,31	0,064	0,05	0,05	Phinney, Simmonds, 1977
Mistactin	20	$6,4 \cdot 10^4$	2,1	18,2	> 12	> 1,8	4) То же
	22	$8,9 \cdot 10^4$	2,3	25,2	12–20	1,8–2,1	"
W. Clearwater	32	$3,2 \cdot 10^5$	3,5	90,2	34–50	2,5–2,9	"
Manicougan	65	$3,5 \cdot 10^6$	7,7	1000	> 600	> 6,6	"
2) Попигайский	75*	$6 \cdot 10^6$	9,1	1630	1750	9,4	5) Масайтис и др., 1975; частное сообщение, 1979
	100**	$1,5 \cdot 10^7$	12,5	4340			

V'_M = Observed melt volume.

*Diameter of a crater in a rocky base.

**Diameter of a crater in a sedimentary cover.

Key: 1) Crater; 2) Popigay; 3) Reference; 4) Ditto; 5) Masaytis et al., 1975; partial publication, 1979.

Analysis shows that calculated melt volumes are somewhat higher than those observed, which is quite understandable if one considers both the indeterminateness of calculating accuracy and the inaccuracy of field observations and data compilations. In addition, one must take into account that part of the melt is ejected from the crater.

Let us evaluate melt zone depth on the Moon. We will use the energy of a crater-forming meteorite as a function of crater diameter (5) and melt zone depth (7) as a function of this energy. Substituting (5) into (7), we obtain

$$z_м = 0{,}05\, D^{1{,}13}. \tag{11}$$

Figure 3 compares this relationship to crater depth and then morphological type as a function of crater diameter. As fig. 3 shows, if crater diameter is greater than 25 km, melt zone

depth becomes greater than apparent crater depth. The primary types of crater involved here are Remer and Tycho. Craters of this type have a bottom whose structure may, in terms of photogeological data, be interpreted as the surface of a solidified shock melt [Howard, Wilshire, 1975].

Thus, one might claim that evaluations of amounts of impact melt based on familiar concepts of the physics and mechanics of hypervelocity impact and explosion agree with data from geological observations. This makes it possible to perform further evaluations on the bases of the relationships derived above for the energy of crater-forming meteorites for attenuation of shock waves beneath the impact point.

Shock Wave Attenuation. Comparison. Calculations of shock wave attenuation for terrestrial meteoric craters can be compared with the level of impact metamorphism of rock, determined in terms of petrographic data. One must keep in mind the distortion of the original relative location of various rock elements when they move during cratering [Dence et al., 1977].

A model has been developed for material flow during crater formation [Ivanov, 1979a, b; Ivanov, Comissarova, 1977; Maxwell, 1977] for simple cup-shaped craters. According to this model, the travel speeds of rock elements found at a certain time at depths z_1 and z_2 under the impact point are related by the ratio /74

$$dz_1/dt = (dz_2/dt)(z_1/z_2)^{-n}. \quad (12)$$

Comparison of (12) with numerical two-dimensional calculations [O'Keefe, Ahrens, 1978] showed that n ranges from 2 to 3. Integrating (12) makes it possible to determine relative soil movements at the axis of symmetry.

$$z_1^{n+1} - z_{10}^{n+1} = z_2^{n+1} - z_{20}^{n+1}, \quad (13)$$

where z_{10} and z_{20} are initial depths of the subject particles. If we known the initial and final positions of a certain reference particle z_{20} and z_2, then with (13) we can easily determine the initial position of any other particle z_1 whose final position we know:

$$z_{10} = (z_1^{n+1} - z_2^{n+1} + z_{20}^{n+1})^{1/(n+1)}. \quad (14)$$

Let us apply this ratio to the crater Brent. We will take as an arbitrary reference particle a unit of soil at the bottom of the melt zone. Its initial depth will be the depth of the melt zone $z_M = z_{20} = 0.31$ km; its final depth, the depth of the foot of the melt lens at the bottom of the crater, $z_2 = 1.08$ km, which is now observable, subtracted from the pre-erosion surface level [Robertson, Grieve, 1977]. Then petrographic data on the level of impact metamorphism, obtained along the core sample from a borehole drilled in the center of the crater Brent [Robertson, Grieve, 1977], may be converted to the initial position at the moment the shock wave passes. Data from this conversion at n = 2 and n = 3 are represented by dots in fig. 7 as compared with theoretical evaluation of shock wave attenuation using equation (6) given a meteorite kinetic energy equal to 230 Mt (table 3):

$$p = 27 z^{-2,7} \quad (15)$$

(here and henceforth, p is expressed in kbar; z, in km).

As figure 7 shows, theoretical analyses and consideration of the shortening of the soil column during crater formation according to (14) correlate poorly with geological data. Comparison of theory and observation shows that rock found in a core sample 85 m thick must be initially located in a layer of soil about 260 m thick, i.e. sideward flow of soil beneath the

crater bottom reduced the initial thickness of the soil layer beneath the crater center almost threefold.

Let us now consider the case of the meteoric crater Kara. Given the crater's observed diameter of D = 50 km [Maslov, 1977], the energy of the meteorite which formed it must, according to equation (2), be about 1.5×10^6 Mt. Then, according to (8), shock wave attenuation is defined by the equation

$$p = 7 \cdot 10^4 z^{-2,7}. \tag{16}$$

Figure 8 shows the position of the calculated function (16) and results of petrographic evaluations (table 2). To make these data correspond, we must assume that rock now at the central uplift was initially at a depth of 10-12 km. The higher observed shock wave attenuation gradient indicates that, as in the case of the crater Brent, movement under the crater center first proceeds downward and is accompanied by lateral flow of rock and a reduction in the length of the soil column under the crater center. Comparison of evaluations and observations shows that column length diminished about threefold during cratering. This is quite similar to the situation with the crater Brent described above.

Note that, if a shock wave 600 m away is to attenuate from 120 to 80 kbar in accordance with petrographic data, the kinetic energy of the meteorite must diminish by a factor of about 15. However, in this case, the rock of the central uplift must have been subjected to a shock pressure at a depth of about 5 km so that it would rise to the observed position, i.e. almost at the original surface level.

Local Gravity Anomalies Related to Craters. A.I. Dabizha and V.V. Fedynskiy [1977] collected a great deal of information on the maximum negative gravity anomaly Δg for terrestrial

meteoric craters. Let us analyze these data using the simplest direct gravimetric problem, i.e. let us set the configuration of the dispersion zone and the extent to which rock disperses in this zone.

As detailed discussions [Dabizha, Ivanov, 1978; Regan, Hinze, 1975] show, dispersion areas under meteoric craters /75
consist of two clearly differentiated zones: a central hemispheric zone beneath the crater and a flattened dish-shaped zone under the crater wall. Since the value of the local gravity anomaly near the crater center is primarily governed by the central dispersion zone, let us approximate it as a hemisphere with a radius equal to the crater's radius $R_B = D/2$. Since the visible crater has a shallow depth for structures larger than several kilometers in diameter, we will disregard correction for relief. Then the negative gravity anomaly near the crater center will equal

$$\Delta g = \pi G \Delta \rho R_B,$$

where G is a gravity constant; $\Delta\rho$, the difference in densities. Let us set $\Delta\rho = 0.1$ g/cm^3, which is typical in order of magnitude for meteoric structures [Regan, Hinze, 1975; Pohl et al., 1977]. Then if we express the magnitude of the anomaly in gravitational force in milligalls (mGal) and the dispersion zone's radius in km, we obtain

$$\Delta g = 1{,}05 D. \qquad (17)$$

This function is depicted in fig. 9 in comparison to observed data. It is clear that it provides a true picture of g for craters with diameters from 3 to 10-20 km. For smaller craters, g is smaller, which may be related to ejection of most of the crushed material outside the crater.

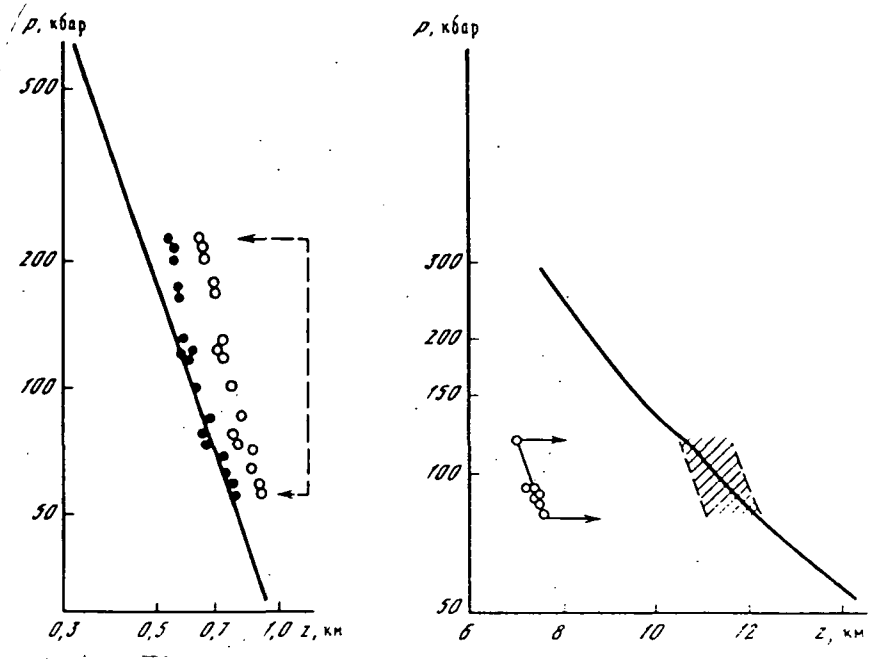

Fig. 7. Attenuation of a shock wave under a crater. Broken line - Apparent relationship between pressure and depth along the soil column [Robertson, Grieve, 1977]; dots, recovery of original position of this column (14) at n = 2 (solid) and n = 3 (hollow). Solid lines, evaluation of (15).

Fig. 8. Evaluation of shock wave attenuation during formation of the crater Kara.
Dots - data from a core sample (table 2) arbitrarily located at a certain absolute depth. Solid lines - evaluation of (16). Shaded area - approximate position of the central peak before impact.

Given a crater diameter of 10-20 km, the depth of our model dispersion zone reaches 5-10 km. For rock density of about 2.5-3 g/cm^3, lithostatic pressure at these depths amounts to $p = pgz \approx 1$-3 kbar. At these ambient pressures, first rock strength increases and, second, rock dispersion becomes more difficult if it is crushed. As shown by observations in deep boreholes and experiments [Simmons et al., 1975; Wang, Simmons, 1978], pressures higher than 1 kbar or depths greater than 5 km

completely close microcracks in rock. Consequently, the dispersion zone of rather large meteoric craters may be enlarged only horizontally as structure diameter increases, remaining approximately constant in depth. The transition from simple to complex gravity anomaly patterns is associated with this effect [Dabizha, Fedynskiy, 1977]. We analyzed anomalies /76 under a dispersed layer of constant depth z_B = 5, 10 km at $\Delta\rho$= 0.1 g/cm^3 using a familiar gravimetric equation

$$\Delta g = 4{,}2 z. \tag{18}$$

These evaluations are illustrated in fig. 9. It is apparent that anomalies Δg for terrestrial craters are of a magnitude no greater than 30 mGal, which completely agrees with the concept that rock at depths beyond a certain limit (5-10 km for Earth) cannot break up or disperse.

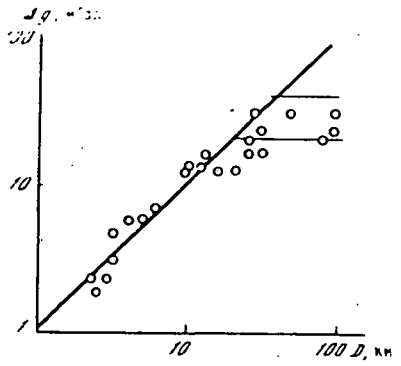

Fig. 9. Negative gravity anomaly amplitude as a function of structure diameter [Dabizha, Fedynskiy, 1977] (dots). The sloped line represents calculation with (17), assuming geometric similarity of dispersion zones. Horizontal line segments represent calculation with (18) at constant dispersion zone depth z_b equal to 10 km (top) and 5 km (bottom).

Since the Moon's gravitational force is one-sixth that of Earth, one might expect that local gravity anomalies above fresh lunar craters would be greater than above terrestrial craters of the same scale. This fact was recently confirmed [Dvorak, Phillips, 1977].

MODELING

The indeterminateness of the mechanical pattern by which central peaks form makes it difficult to model this process. We performed two preliminary experiments, assigning an important role to the margin of elastic deformations in rock near a growing crater. Geological literature often calls this mechanism of central peak formation "elastic recoil."

"Rubber sand" consisting of finely chopped pieces of sponge rubber measuring about 2-3 mm was prepared. A hypervelocity impact was simulated by exploding a charge of 0.4 g TNT. The rubber sand was poured into a flat layer bounded on one side by a plexiglass window, which made it possible to observe the motion of the substance in a plane crossing the charge [Ivanov, 1979a, b]. A similar procedure was used in [Piecutowsky, 1977]. Plastic disks -- markers measuring 3 and 5 mm -- were placed in the sand. These disks made it possible to determine the trajectory of soil particle travel. Because the rubber was black, the pattern of sand motion was invisible on movie film, but the motion of the markers was easily tracked.

Figure 10 shows the general view of the depression which formed (the central peak formed beneath the center of the explosion was quite noticeable); figure 11 a, the trajectory of marker movement in this experiment. It was clear that near-surface markers fly just as they do in ordinary sand (fig. 11 c), while the motion of immersed markers is clearly divided into two stages: nearly radial displacement from the center of the explosion, and "elastic" recoil upward and from the center, which was followed by free flight in the gravitational field.

The goal of the second experiment was to improve the visibility of the rubber sand on movie film. It was mixed with white talcum powder (in proportion of approximately 30:1).

Visibility on movie film barely improved, but the final depression in this experiment assumed a normal cup shape (fig. 12). Marker trajectories in this experiment (fig. 11 b) were quite similar to those in the first experiment (fig. 11 a): near-surface markers moved just as in ordinary sand, while those immersed after rapid radial displacement from the center experienced "elastic recoil."

Qualitative analysis of the properties of the medium used in the first and second experiments showed that adding talc greatly reduced the rubber sand's shear strength. It seems to us that this circumstance was key in the experiments described /77
above: in the first experiment, high adhesion among rubber sand particles prevented the material, which had built up high elastic deformation reserves, from spreading. Discharging this material and removing elastic deformations also resulted in formation of a central uplift. In the second experiment, talcum powder reduced adhesion, and the material, which had stored elastic deformations, spread sideward. Although discharging it also led to "elastic recoil" in part of the substance, it could not form a central peak.

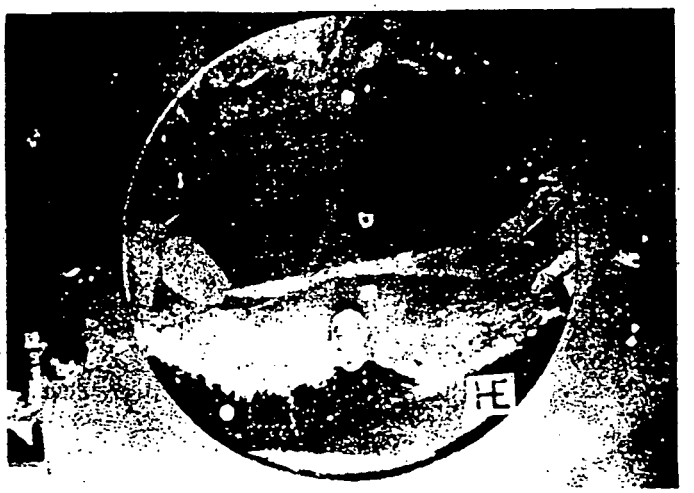

Fig. 10. General view of the cross section of a contact explosion depression in "rubber sand" with clear central uplift. The diameter of the round window was 30 cm. The inner surface of the crater was coated at the top with talc to highlight the cross section profile.

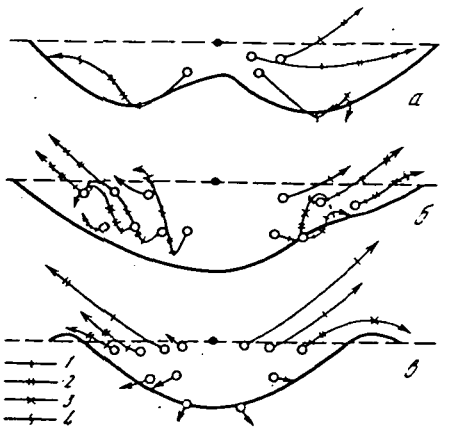

Fig. 11. Marker trajectories during crater formation in (a) "rubber sand," (b) a "rubber sand"-talc mixture, and (c) ordinary dry sand.
Solid dots represent the position of the explosive charge. Marks on trajectories denote: 1) 8 m/sec; 2) 16; 3) 32; 4) 64. Final crater diameters relative to the initial surface level (broken line): a) 35; b) 33, and c) 25 cm.

This intuitive picture of the process must certainly be supplemented by measurements of medium properties and, of course, much more extensive experimental data. Note that use of rubber sand made it possible for the first time to observe the development of a central peak in a uniform laboratory massif, which inarguably provides certain guidelines for planning future experiments.

DISCUSSION

1. The discussions introduced above, based on traditional concepts of cratering, led to the conclusion that there is a significant vertical uplift of part of the crater bottom during formation of a central uplift.

The first prerequisite for this conclusion is the observed elevation of rock in craters formed in stratified targets (see table 1). This uplift may be measured in terms of the depths of deposition of the same rocks outside the crater and in the central peak. The difference between these depths governs the amplitude of the uplift of rock in the central peak above the initial deposition level. These data are shown in fig. 13 as

uplift amplitude vs. structure diameter (double dots).

The second method of evaluating uplift amplitude involves comparing the observed depth of the apex of the central peak relative to the initial surface level and calculated melt zone depth. As noted in the section "Observations," central peak rock never shows traces of impact melting, and this means that, in the initial deposit, these rocks lie below the level now observed. Melt zone depth can be evaluated both by calculation and mentally by collecting the quantity of the melt observed in craters in a hemisphere bounded by the isobar of impact pressure equal to the pressure at which the rock melts (see table 3). Evaluations of uplift amplitude in terms of the observable amount of impact melting as a function of crater diameter appear in fig. 13 (dots). Uplift amplitude, assuming rock uplift from a depth equal to calculated melt zone depth z_M (see equation (8)) at the initial surface level, is calculated and expressed in fig. 13 as a solid line. /78

Fig. 12. General view of the depression in a "rubber sand"-talc mixture.
No central uplift.

The third evaluation method is based on the observed magnitude of impact metamorphism in rock at the top of the central uplift. At the crater Kara (see table 2) and at other structures [Robertson, 1975; Robertson, Grieve, 1977], petrographic changes in central uplift rock did not exceed

changes typical for shock wave pressures on the order of 300 kbar. Figure 13 shows the depth below the center at which this pressure is achieved in an attenuating shock wave as a function of creater diameter as a broken line.

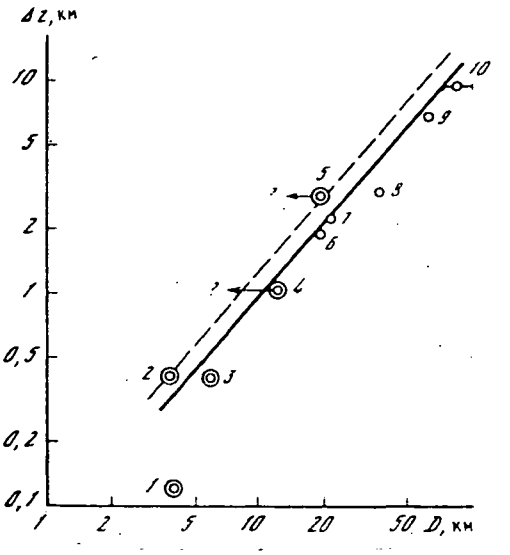

Fig. 13. Various evaluations of rock uplift amplitude in a central uplift.
Double dots - craters in stratified targets (see table 1): 1) Steinheim; 2) Flynn Creek; 3) Decaturville; 4) Sierra Madera; 5) Gosses Bluff. Dots - evaluations in terms of the radius of a hemisphere with a volume equal to that of the observed shock melt (see table 3, z_M'): 6) Mistactin; 7) Boltyshsk; 8) W. Clearwater; 9) Manicougan; 10) Popigay. For maximum evaluation, it was assumed that the foot of the melt zone or rocks exposed to impact compression to 300 kbar are raised in the central uplift approximately to the level of the original surface.

As figure 13 clearly shows, all these methods for evaluating uplift amplitude yield similar relationships between amplitude and structure diameter. The data introduced might lead one to conclude that, given a crater diameter larger than 4 km, rock in the center of a crater after the initial stage of cratering, which may take place similarly in larger craters

(with formation of cup-shaped intermediate depression), experiences a vertical uplift with an amplitude of about one-tenth the crater's diameter. This indicates that, in craters /79
the size of Manicougan or Poligay (their diameters are 80 and 100 km respectively), rock previously deposited at a depth of about 7-10 km rises to the surface.

One can arrive at similar conclusions by comparing the estimated depth of the melt zone in lunar craters and the position of the apex of the central peak in them, since photogeological data indicate that central peaks in lunar craters did not melt during meteorite impact (see fig. 4 and 5).

2. Evaluation of typical time for a melt to harden in large terrestrial craters (about 100 sec) [Phinney, Simmonds, 1977] makes it possible to determine the rate at which central peaks rise. If, according to data from observations at all meteoric craters on Earth, the melt must be able to flow from the central peak until it hardens, this means that a 5-10-km uplift takes about as much time as it does for the melt to solidify, i.e. about 100 sec. This results in an estimate of the average rate of uplift of about 50-100 m/sec, which demonstrates the highly dynamic nature of this process.

The mechanism proposed earlier for formation of a central uplift with matter from the mantle flowing under the crater should have a typical time of about 10^3-10^4 years [Dabizha et al., 1976], which does not correlate with the lack of impact melts at the apices of central uplifts.

3. Formation of central peaks in impact craters in stratified targets has frequently been observed when there is a stronger substrate layer [Quide, Oberbek, 1977]. The central peak consists of material virtually unmoved from its initial position, both horizontally and vertically. Extrapolation of

this mechanism to larger craters [Head, 1976] is unjustified in view of the data presented above.

4. The reasons for the considerable uplift of rock at crater centers still remain unclear. The structure of a planet core sample cannot be the only cause of this process, since craters on the "stiff," confining mascons of the Moon exhibit the same sequence of change in crater structure as diameter increases as do craters on the "plastic," isostatic, compensated Earth.

5. Primitive modeling of crater formation in a highly elastic medium has shown that elastic recoil of a substance near the crater bottom can cause upward movement. The margin of reversible deformations in sub-crater material can be controlled by the substance's shear strength, as indicated earlier by analysis of the formation of a central peak in an experimental crater formed by contact explosion of a charge in rocky soil [Ulrich et al., 1977]. In the case of large meteoric craters, lithostatic pressure, which plays a much smaller role in formation of small cup-shaped craters which do not exhibit central peaks, may be a factor which increases the shear strength of rock beneath a crater. The fact that gravity anomaly amplitude is unrelated to crater size (at diameters near or above 10-20 km for terrestrial craters) may prove the effect of lithostatic pressure on breakup of rock under large meteoric craters.

CONCLUSION

Through analysis of theoretical, experimental, and field data, this article proves the presence of a significant uplift of rock above its initial level of deposition during formation of central uplifts in large meteoric craters. The significant feature of this phenomenon is the presence of a critical crater

size which differs on different planetary bodies. This separates the range of crater dimensions in which a central uplift does and does not form. In future theoretical and experimental study of the process of central uplift (peak) formation in meteoric craters, hardening of rock at a certain depth when exposed to lithostatic pressure must be studied and appropriate model experiments conducted.

The authors are grateful to their colleagues for their considerable assistance, especially K.P. Florenskiy for suggesting the general idea for this work; V.L. Masaytis, for discussing the structure of large terrestrial meteoric craters; N.N. Bobina, L.L. Comissarova, and V.P. Shashkina, for assistance in producing the "rubber sand;" and L.B. Granovskiy, for organizing field work at the crater Kara.

In Russian:

Bazilevskiy, A.T., Ivanov, B.A., "Review of Achievements in Crater Formation Mechanics," in Mekhanika obrazovaniya voronok pri udare i vzryve, [Mechanics of Depression Formation upon Impact and Explosion]. Moscow: Mir Press, 1977, pp. 172-227.

Dabizha, A.I., Krass, M.S., Fedynskiy, V.V. "Evolution of Meteoric Craters as Structures of the Earth's Core," Astron. vestn., 1976, vol. 10, No. 1, pp. 6-18.

Dabizha, A.I., Fedynskiy, V.V., "Features of Astrobleme Gravitational Fields," Meteoritika, 1977, No. 36, pp. 113-119.

Dabizha, A.I., Ivanov, B.A., Geophysical Model of the Structure of Meteoric Craters and Certain Problems of Crater-Formation Mechanics," Meteoritika, 1978, No. 37, pp. 160-167.

Dence, M.R., "Extraterrestrial Origin of Canadian Craters," in Vzryvnyye kratery na Zemle i planetakh [Explosive Craters on the Earth and Planets]. Moscow: Mir Press, 1968, pp. 105-129.

Ivanov, B.A., "Certain Problems in the Mechanics of Impact and Explosion Crater Formation," in Meteoritnyye struktury na poverkhnosti planet [Meteoric Structures on Planet Surfaces]. Moscow: Nauka Press, 1979a, pp. 31-45.

Ivanov, B.A., "A Simple Model of Cratering," Meteoritika, 1976b, No. 38, pp. 68-85.

Masaytis, V.L., Mikhaylov, M.V., Selivanovskaya, T.V., Popigayskiy Meteoritnyy Krater [Popigay Meteor Crater]. Moscow: Nauka Press, 1975, 125 pp.

Masaytis, V.L., "Morphology and Structure of Impact Craters and Astroblemes," Letter to Astron. zhurn., 1977, No. 3, pp. 36-39.

Maslov, M.A., "On the Origin of the Kara Depression," Meteoritika, 1977, No. 36, pp. 123-130.

Oberbek, V.R., "Laboratory Modeling of Impact Crater Formation using Explosive Substances," in Mekhanika obrazovaniya voronok pri udare i vzryve [Mechanics of Depression Formation During Impact and Explosion]. Moscow: Mir Press, 1977, pp. 33-61.

O'Keefe, J.D., Ahrens, T.J., "Impact Effects during Collision of Large Meteorites with the Moon," in Mekhanika obrazovaniya voronok pri udare i vzryve [Mechanics of Depression Formation

During Impact and Explosion]. Moscow: Mir Press, 1977, pp. 62-79.

Quide, Y.L. Oberbek, V.R., "Determination of the Thickness of the Surface Layer of the Moon in Terms of Impact Craters, in Mekhanika obrazovaniya voronok pri udare i vzryve [Mechanics of Depression Formation During Impact and Explosion]. Moscow: Mir Press, 1977, pp. 86-129.

Shumeyker, Yu.M., "Mechanics of Impact in the Example of the Arizona Meteor Crater," in Vzryvnyye kratery na Zemle i planetakh [Explosive Craters on the Earth and Planets]. Moscow: Mir Press, 1968, pp. 68-104.

Yurk, Yu.Yu., Yeremenko, G.K., Polkanov, Yu. A., "The Boltyshsk Depression -- A Ridged Meteor Crater," Sov. geol., 1975, No. 2, pp. 138-144.

In English:

Ahrens, T.J., O'Keefe, J.D., "Equations of State and Impact-Induced Shock-Wave Attenuation on the Moon, in Impact and Explosion Cratering. New York: Pergamon Press, 1977, pp. 639-656.

Allen, R.C., "Central Peaks in Lunar Craters," Moon, 1975, vol. 12, No. 4, pp. 463-474.

Baldwin, R.B., The Measure of the Moon. Chicago: Univ. Chicago Press, 1963. 488 pp.

Bjork, R.L., "Analysis of the Formation of Meteor Crater, Arizona: A Preliminary Report," J. Geophys. Res., 1961, vol. 66, No. 10. pp. 3379-3387.

Controlled Mosaics of the Yorktown Region of Mars (Viking I Landing Site), U.S.G.S. map 1-1059, 1977.

Dence, M.R., Grieve, R.A.F., Robertson, R.B., "Terrestrial Impact Structures: Principal Characteristics and Energy Considerations," in Impact and Explosion Cratering. New York: Pergamon Press, 1977, pp. 247-275.

Dienes, J.K., Walsh, J.M., "Theory of Hypervelocity Impact," Systems, Sciences, and Software Report 3SlR-676. Calif., 1969.

Dvorak, J., Phillips, R.J., "The Nature of the Gravity Anomalies Associated with Large Young Craters," Geophys. Res. Lett., 1977, vol. 4, No. 9, pp. 380-382.

Florensky, C.P., Basilevskiy, A.T., Grebennik, N.N., "The Relationship Between Lunar Crater Morphology and Crater Size,"

Moon, 1976, vol. 16, No. 1, pp. 59-70.

Gault, D.E., Guest, J.E., Murray, J.B. et al., "Some Comparisons of Impact Craters on Mercury and on the Moon," J. Geophys. Res., 1975, vol. 80, No. 87, p. 2444-2460.

Gault, D.E., Wedekind, J.A., "Experimental Hypervelocity Impact into Quartz Sand. II: Effects of Gravitational Acceleration," in Impact and Explosion Cratering. New York: Pergamon Press, 1977, pp. 1231-1244.

Head, J.W., "The Significance of Substrate Characteristics in Determining Morphology and Morphometry of Lunar Craters," in Lunar Science VII. Houston: Lunar Sci. Inst., 1976, pp. 354-356.

Howard, K.A., Wilshire, H.G., "Flow of Impact Melt at Lunar Craters," J. Res. U.S. Geol. Surv., 1975, vol. 3, No. 2, pp. 237-251.

Ivanov, B.A., "The Effect of Gravity on Crater Formation: Thickness of Ejecta and Concentric Basins," in Proc. Lunar Sci. Conf. 7th. New York: Pergamon Press, 1976, pp. 2947-2965.

Ivanov, B.A., Comissarova, L.I., "The Simple Hydrodynamic Model of Cratering," in Lunar Science VIII. Houston: Lunar Sci. Inst., 1977, pp. 499-501.

Johnson, S.W., Smith, J.A., Franklin, E.G. et al., "Gravity and Atmospheric Pressure Effects on Crater Formation in Sands," J. Geophys. Res. 1969, vol. 74, No. 20, pp. 4838-4850.

Offield, T.W., Pohn, H.A., "Deformation at the Decaturville Impact Structure, Missouri," in Impact and Explosion Cratering. New York: Pergamon Press, 1977, pp. 321-341.

O'Keefe, J.D., Ahrens, T.J., "Late Stage Crater Flows and the EFfect of Strength on Transient Crater Depth," in Lunar and Planetary Sciences IX. Houston: Lunar and Planet. Sci. Inst., 1978, pp. 823-825.

Maxwell, D.E., "Simple Z-model of Cratering, Ejection and Overturned Flap," in Milton, D.J., Barlow, B.C., Brett, R. et al., "Gosses Bluff Impact Structure, Australia," Science, 1972, vol. 175, No. 4027, pp. 1199-1207.

Piecutowski, A.J., "Cratering Mechanisms Observed in Laboratory Scale High-Explosive Experiments," in Impact and Explosion Cratering. New York: Pergamon Press, 1977, pp. 67-102.

Phinney, W.C., Simonds, C.H., "Dynamic Implications of the Petrology and Distribution of Impact Melt Rock," in Impact and /81

Explosion Cratering. New York: Pergamon Press, 1977, pp. 771-790.

Pohl, J., Stoffler, D., Gall, H., Ernston, K., "The Ries Impact Crater," in Impact and Explosion Cratering. New York: Pergamon Press, 1977, pp. 343-404.

Regan, R.D., Hinze, W.J., "Gravity and Magnetic Investigations of Meteor Crater, Arizona," J. Geophys. Res., 1975, vol. 80, No. 5, pp. 776-788.

Reiff, W., "The Steinheim Basin -- An Impact Structure," in Impact and Explosion Cratering. New York: Pergamon Press, 1977, pp. 309-320.

Robertson, P.B., "Zones of Shock Metamorphism at the Charlevoix Structure, Quebec," Bull. Geol. Soc. Amer., 1975, vol. 86, No. 12, pp. 1630-1638.

Robertson, P.B., Grieve, R.A.F., "Shock Attenuation at Terrestrial Impact Craters," in Impact and Explosion Cratering. New York: Pergamon Press, 1977, pp. 687-702.

Roddy, D.J., "Tabular Comparisons of the Flynn Creek Impact Crater, U.S., Steinheim Impact Crater, Germany, and Snowball Explosion Crater, Canada," in Simmons, G., Siegfried, R., Richter, D., "Characteristics of Microcracks in Lunar Samples," in Proc. Lunar Sci, Conf. 6th. New York: Pergamon Press, 1977, pp. 125-162.

Ullrich, G.W., Roddy, D.J., Simmons, G., "Numerical Simulation of a 20-Ton TNT Detonation on the Earth's Surface and Implications Concerning the Mechanics of Central Uplift Formation," in Impact and Explosion Cratering. New York: Pergamon Press, 1977, pp. 959-983.

Wang, H.T., Simmons, G., "Microcracks in Crystalline Rock from 5.3-km Depth in the Michigan Basin," J. Geophys. Res., 1978, vol. 83, NB12, pp. 5849-5856.

Wood, C.A., Cintala, M.J., Head, J.W., "Interior Morphometry of Fresh Martian Craters: Preliminary Viking Results," in Lunar and Planetary Sciences IX. Houston: Lunar and Planet. Sci. Inst., 1978, pp. 1270-1272.

STANDARD TITLE PAGE

1. Report No.	2. Government Accession No.	3. Recipient's Catalog No.
NASA TM-88427		

4. Title and Subtitle	5. Report Date
FORMATION OF THE CENTRAL UPLIFT IN METEORITE CRATERS	MAY 1986
	6. Performing Organization Code

7. Author(s)	8. Performing Organization Report No.
Ivanov, B.A.; Bazilevskiy, A.T.; Sazonova, L.V.	10. Work Unit No.

9. Performing Organization Name and Address	11. Contract or Grant No.
The Corporate Word 1102 Arrott Building Pittsburgh, PA 15222	NASW-4006
	13. Type of Report and Period Covered
	Translation
12. Sponsoring Agency Name and Address	14. Sponsoring Agency Code
National Aeronautics and Space Administration Washington, D. C. 20546	

15. Supplementary Notes

Translation of "Ob obrazovanii tsentral'nogo podnyatiya v v meteoritnykh krateraklh," IN: Meteoritika, Akademiya Nauk SSSR, No. 4, 1982, pp. 67-81 (82A47141) (UDC 523.681.8 : 550.311)

16. Abstract

Data are presented on the sizes of impact craters with central uplifts on the earth, moon, and terrestrial planets. It is proposed that the central uplift of the Kara crater in the USSR was formed by impactt metamorphism of rocks along a crater having a depth of about 600 meters. A theoretical analysis of the mechanics of hypervelocity impact cratering is used to investigate the features of shock-wave attenuation in the depths of the target and the amount of impact melt formed during this process. An attempt is made to determine the velocity of rock motion during the formation of central uplifts in terrestrial craters.

17. Key Words (Selected by Author(s))	18. Distribution Statement
	Unlimited

19. Security Classif. (of this report)	20. Security Classif. (of this page)	21. No. of Pages	22. Price
Unclassified	Unclassified	33	

NASA-HQ